Bed nuclei of the stria terminalis modulate memory consolidation via glucocorticoid-dependent and -independent circuits

Ryan T. Lingg[a], Shane B. Johnson[b], Eric B. Emmons[b], Rachel M. Anderson[a], Sara A. Romig-Martin[a], Nandakumar S. Narayanan[b,c,d], James L. McGaugh[e,f,1], Ryan T. LaLumiere[a,b,d,1], and Jason J. Radley[a,b,d,1]

[a]Department of Psychological and Brain Sciences, University of Iowa, Iowa City, IA 52242; [b]Interdisciplinary Neuroscience Program, University of Iowa, Iowa City, IA 52242; [c]Department of Neurology, Carver College of Medicine, University of Iowa, Iowa City, IA 52242; [d]Iowa Neuroscience Institute, University of Iowa, Iowa City, IA 52242; [e]Center for the Neurobiology of Learning and Memory, University of California, Irvine, CA 92697-3800; and [f]Department of Neurobiology and Behavior, University of California, Irvine, CA 92697-3800

Contributed by James L. McGaugh, February 11, 2020 (sent for review September 11, 2019; reviewed by Keng Chen Liang and Carmen Sandi)

There is extensive evidence that glucocorticoid hormones enhance memory consolidation, helping to ensure that emotionally significant events are well remembered. Prior findings suggest that the anteroventral region of bed nuclei of the stria terminalis (avBST) regulates glucocorticoid release, suggesting the potential for avBST activity to influence memory consolidation following an emotionally arousing learning event. To investigate this issue, male Sprague-Dawley rats underwent inhibitory avoidance training and repeated measurement of stress hormones, immediately followed by optogenetic manipulations of either the avBST or its projections to downstream regions, and 48 h later were tested for retention. The results indicate that avBST inhibition augmented posttraining pituitary–adrenal output and enhanced the memory for inhibitory avoidance training. Pretreatment with a glucocorticoid synthesis inhibitor blocked the memory enhancement as well as the potentiated corticosterone response, indicating the dependence of the memory enhancement on glucocorticoid release during the immediate posttraining period. In contrast, posttraining avBST stimulation decreased retention yet had no effect on stress hormonal output. Subsequent experiments revealed that inhibition of avBST input to the paraventricular hypothalamus enhanced stress hormonal output and subsequent retention, whereas stimulation did not affect either. Conversely, stimulation—but not inhibition—of avBST input to the ventrolateral periaqueductal gray impaired consolidation, whereas neither manipulation affected glucocorticoid secretion. These findings indicate that divergent pathways from the avBST are responsible for the mnemonic effects of avBST inhibition versus stimulation and do so via glucocorticoid-dependent and -independent mechanisms, respectively.

inhibitory avoidance | contextual fear | ventrolateral periaqueductal gray | HPA axis | paraventricular nucleus of the hypothalamus

Emotionally arousing experiences produce lasting memories (1, 2), an effect mediated, at least in part, by activation of adrenal stress hormones, including cortisol (corticosterone, or CORT, in rodents) and epinephrine (3–9). These hormones influence memory consolidation processes that occur during the immediate postlearning period and depend on the basolateral amygdala (BLA) for their memory-modulatory effects. For example, amygdala lesions or noradrenergic receptor blockade in the amygdala prevent the memory-enhancing effects of systemically administered CORT and epinephrine (10–14). The BLA, in turn, modulates memory consolidation through its interactions with other brain regions, including the bed nuclei of the stria terminalis (BST). Prior work has indicated that the memory-modulatory ability of the amygdala depends on concurrent activation of the BST (15–17), suggesting that the BST acts "downstream" from the amygdala in influencing memory consolidation.

The BST is a complex of heterogeneous regions with distinct functions (18–22). Whereas previous studies focused on the dorsal BST, findings from our laboratory suggest that a different subregion, the anteroventral subdivision (avBST), regulates the acute behavioral and physiological responses to stressors and emotional arousal (23, 24). The avBST is well-positioned to modulate neuroendocrine responses to stress (25–29). It provides a GABAergic input to effector neurons in the paraventricular hypothalamic nucleus (PVH) that modulate the hypothalamic–pituitary–adrenal (HPA) axis and thereby regulate peripheral glucocorticoid levels in response to a variety of aversive experiences (22, 23, 30–32). Thus, avBST and its projections to the PVH may serve as a critical central regulator of CORT release during the posttraining period of memory consolidation. The avBST also projects to the periaqueductal gray (PAG) (24, 33, 34), and recent findings implicate the PAG more directly in memory consolidation following aversive experiences, either itself as a nodal point or as a relay to limbic cortical consolidation networks (35–38).

Together, these findings suggest a rather distinct role for the avBST, compared to the dorsal regions of BST previously investigated. To address this issue, the present study used an optogenetic approach in rats to control activity of avBST neurons and its projections to the PVH and ventrolateral PAG following training in a single-trial inhibitory avoidance (IA) task. CORT and adrenocorticotropic hormone (ACTH) levels were assessed before and after training. Rats' retention of IA learning was measured 2 d after training. The findings indicate that the

Significance

Memory consolidation following emotionally significant events is enhanced by glucocorticoid hormones. Our report identifies the anteroventral bed nuclei of the stria terminalis (avBST) as capable of bidirectionally modulating memory consolidation in rats following inhibitory avoidance learning. Follow-up experiments revealed that divergent pathways from avBST are responsible for the mnemonic effects of avBST inhibition and stimulation and that they occur via glucocorticoid-dependent and -independent mechanisms, respectively.

Author contributions: R.T. Lingg, N.S.N., J.L.M., R.T. LaLumiere, and J.J.R. designed research; R.T. Lingg, S.B.J., E.B.E., R.M.A., S.A.R.-M., N.S.N., and J.J.R. performed research; R.T. Lingg, S.B.J., E.B.E., N.S.N., and J.J.R. analyzed data; and R.T. Lingg, J.L.M., R.T. LaLumiere, and J.J.R. wrote the paper.

Reviewers: K.C.L., National Taiwan University; and C.S., Ecole Polytechnique Federale de Lausanne.

The authors declare no competing interest.

[1]To whom correspondence may be addressed. Email: james.mcgaugh@uci.edu, ryan-lalumiere@uiowa.edu, or jason-radley@uiowa.edu.

This article contains supporting information online at https://www.pnas.org/lookup/suppl/doi:10.1073/pnas.1915501117/-/DCSupplemental.

First published March 19, 2020.

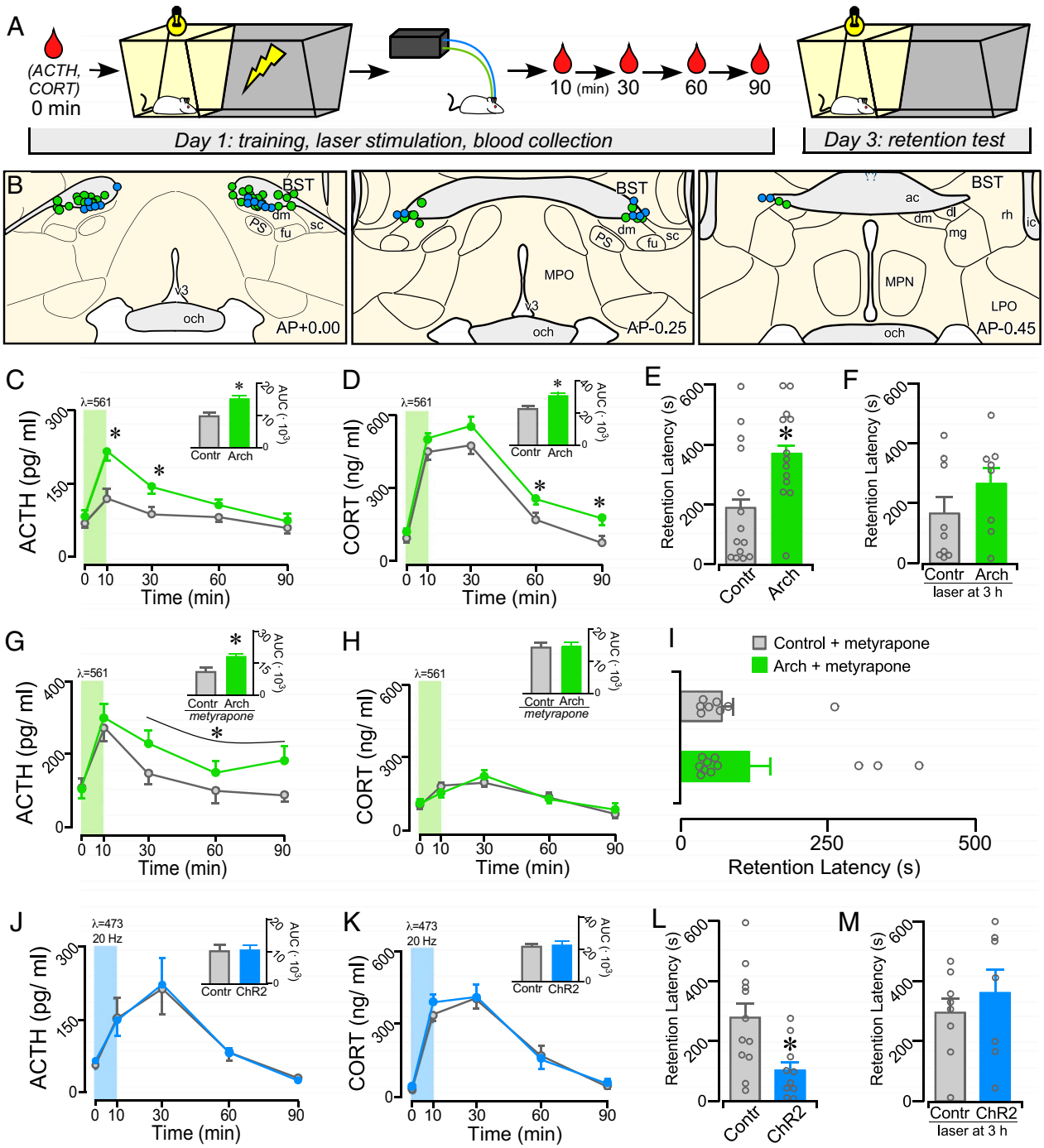

Fig. 1. Posttraining manipulation of avBST activity bidirectionally modulates IA memory consolidation. (*A*) Diagram illustrating the experimental time line. Posttraining inhibition and stimulation of the avBST were conducted in serial experiments and were compared with AAV5-YFP control rats receiving identical illumination, respectively. (*B*) Examples of fiber optic implants targeted toward the region immediately dorsal to the avBST for illumination. Circles represent rats from separate experiments, first for Arch inhibition (green, $n = 13$; $n = 11$ for metyrapone + Arch group in *G*–*I*), and next for ChR2 activation (blue, $n = 10$) of avBST neurons. Coronal atlas images adapted from Swanson (93). (*C* and *D*) Shown are mean ± SEM of plasma ACTH (*C*) and CORT (*D*) in control and Arch groups before (0 min) and at various intervals following IA training. Both hormones are significantly increased in the Arch group at various intervals following illumination. (*C* and *D*, *Inset*) Integrated ACTH and CORT responses (AUC) were also significantly increased in the Arch versus YFP groups. (*E* and *F*) Inhibition of avBST neurons in the Arch group immediately posttraining increased retention latencies when measured 48 h later (*E*), but not when inhibition was administered 3-h posttraining (*F*). (*G* and *H*) Mean ± SEM of plasma ACTH and CORT in control and Arch groups before (0 min) and at various intervals following IA training following pretreatment with a glucocorticoid synthesis blocker (metyrapone). Inhibition of avBST with Arch potentiated the increase in plasma ACTH levels, whereas CORT levels were not distinguishable between Arch and control groups due to pretreatment with metyrapone. (*G* and *H*, *Inset*) Integrated ACTH and CORT responses (AUC) in Arch and YFP groups. (*I*) Posttraining inhibition of avBST neurons failed to enhance retention latencies when assessed 48 h later. (*J* and *K*) Plasma levels of ACTH (*J*) and CORT (*K*) were not significantly altered by posttraining activation of avBST neurons with ChR2. (*L* and *M*) ChR2 rats displayed significantly decreased retention latencies relative to YFP controls (*L*) when assessed 48 h later, whereas stimulation with ChR2 at 3-h posttraining had no effect (*M*). *$P < 0.05$. ac, anterior commissure; dl, BST dorsolateral subdivision; dm, avBST dorsomedial subdivision; fu, avBST fusiform subdivision; LPO, lateral preoptic area; mg, BST magnocellular subdivision; MPN, median preoptic nucleus; MPO, medial preoptic area; och, optic chiasm; PS, parastrial nucleus; rh, BST rhomboid subdivision; sc, avBST subcommissural subdivision.

avBST→PVH and avBST→ventrolateral PAG pathways are capable of modulating memory consolidation, via glucocorticoid-dependent and -independent mechanisms, respectively.

Results

avBST Bidirectionally Modulates Memory Consolidation via HPA-Dependent and -Independent Mechanisms. Adult male Sprague-Dawley rats received microinjections in avBST with adeno-associated virus (AAV5) containing the inhibitory opsin-enhanced archaerhodopsin 3.0 or excitatory channelrhodopsin-2 (E123A) (Arch and ChR2, respectively) (39, 40), both fused to enhanced yellow fluorescent protein (YFP) and under the human synapsin-1 promoter. These injections were targeted to produce expression in a population of GABAergic projection neurons within the division of BST considered as "ventrolateral" by Alheid and Heimer (41) and De Olmos et al. (42) or within fusiform, dorsomedial, and subcommissural subdivisions according to the nomenclature of Dong and Swanson (33, 34). Designation of this BST region as "anteroventral" is based upon these different taxonomic regimes and its exclusivity from other BST regions dorsal and posterior to the anterior commissure. In order to activate or inactivate neuronal cell bodies, optical fibers were implanted above the avBST (Fig. 1*A*). IA training consisted of a standard IA apparatus, in which the rat was placed into a brightly lit compartment, and then upon crossing into the darkened compartment, received a single inescapable footshock (0.8 mA, 1-s duration). In an initial experiment (Fig. 1*B*), rats expressing either Arch or YFP in avBST received illumination of avBST for 10 min with 561-nm light immediately after IA training. Blood samples were collected from indwelling jugular catheters in both groups immediately prior to training (0 min) and at 10, 30, 60, and 90 min posttraining.

Radioimmunometric analysis of plasma levels of ACTH and CORT revealed posttraining increases in both groups, with Arch rats displaying a greater enhancement relative to YFP controls. For ACTH, repeated-measures ANOVA revealed an interaction between group and time ($F_{4, 92} = 3.32$, $P = 0.014$) and main effects of group ($F_{1, 23} = 14.89$, $P = 0.001$) and time ($F_{4, 92} = 17.54$, $P < 0.001$). Posttraining avBST inhibition increased integrated ACTH responses (area under curve, AUC; $t_{23} = 3.43$, $P = 0.002$) and increased ACTH levels at 10 and 30 min ($P = 0.003$ and 0.012, respectively) relative to the YFP control values (Fig. 1*C*). Analysis of plasma CORT revealed main effects of group ($F_{1, 23} = 7.71$, $P = 0.011$) and of time ($F_{4, 92} = 101.34$, $P < 0.001$) (no group-by-time interaction). Posttraining avBST inhibition produced an increased integrated CORT response (AUC; $t_{23} = 2.92$, $P = 0.008$) and increased CORT levels at 60- and 90-min time points ($P = 0.016$ and 0.040, respectively), as compared with YFP control rats (Fig. 1*D*). Two days after training, rats were assessed for IA retention by being placed back in the lit compartment, and their latency to enter the darkened compartment was utilized as an index of retention. Rats that had received avBST inhibition displayed significantly higher retention latencies compared to YFP controls ($t_{25} = 2.50$; $P = 0.019$) (Fig. 1*E*). To address the possibility that posttraining inhibition produced long-lasting changes in avBST that account for the altered retention, an additional group of rats expressing Arch or YFP received a 10-min illumination period of avBST 3 h after IA training. However, there was no significant difference in the retention latencies between the groups (Fig. 1*F*).

Given that posttraining administration of glucocorticoids has been shown to enhance memory for IA training (13, 43, 44), the memory modulatory effect of avBST inactivation may be regulated through its potentiating effects on adrenocortical output. To address this possibility, a follow-up experiment was carried out repeating the same design as shown in Fig. 1*B*, except both groups of rats received pretreatment with the CORT synthesis inhibitor, metyrapone, 90 min before IA training. Previous work indicates that a 50 mg/kg (subcutaneous) dose of metyrapone given 90 min prior to IA training attenuates the induction of glucocorticoids without altering retention on its own (45). IA training significantly increased ACTH levels, with potentiation of this response in rats receiving avBST inhibition with Arch (Fig. 1*G*). A repeated-measures ANOVA revealed a main effect for time ($F_{4, 56} = 4.82$, $P = 0.002$) and a nonsignificant trend for avBST inhibition to potentiate the ACTH response ($F_{1, 14} = 4.21$, $P = 0.059$; no group-by-time interaction). Additionally, avBST significantly increased integrated ACTH values compared to YFP controls ($t_{14} = 2.43$, $P = 0.029$). However, metyrapone blunted the CORT response following IA training and prevented its potentiation following avBST inhibition (Fig. 1*H*). Repeated-measures ANOVA revealed a main effect only for time ($F_{4, 60} = 14.92$, $P = 0.001$), but not for group ($F_{4, 60} = 0.1$, $P = 0.8$), interaction ($F_{4, 60} = 0.6$, $P = 0.6$), or effect of inhibition on integrated CORT (AUC: $t_{15} = 0.1$, $P = 0.9$). Moreover, metyrapone pretreatment prevented the retention-enhancing effects following avBST inhibition, as retention latencies did not significantly differ between Arch-expressing and YFP control rats (Fig. 1*I*).

The next experiment involved activating the avBST in rats expressing either ChR2 or YFP for 10 min with 473-nm light (20 Hz, 5-ms pulse width), immediately following IA training. For this, the shock amplitude was increased (1.0 mA, 2 s) to ensure sufficiently high retention latencies to observe impairments in retention (46–49), as the foregoing results suggest that posttraining stimulation of avBST may attenuate retention. As before, IA training significantly increased plasma CORT and ACTH in both groups, as indicated by main effects of time (ACTH: $F_{4, 76} = 14.84$, $P < 0.001$; CORT: $F_{4, 76} = 84.55$, $P < 0.001$). However, no main effects of group (ChR2 vs. YFP controls) or interaction were observed, nor were any differences found in integrated values for either ACTH or CORT (Fig. 1 *J* and *K*). Nevertheless, rats receiving avBST stimulation with ChR2 had significantly attenuated retention latencies compared to YFP controls ($t_{20} = 2.90$; $P = 0.009$) (Fig. 1*L*). As with the optical inhibition experiment, a control experiment was conducted in which rats expressing either ChR2 or YFP in avBST received the same laser illumination (20 Hz for 10 min) 3 h after IA training. However, there was no significant difference in the retention latencies between the groups (Fig. 1*M*). Altogether, the findings of these initial experiments indicate that the mnemonic effects of avBST inhibition versus stimulation occur via glucocorticoid-dependent and -independent mechanisms, respectively.

Opsin functionality was verified in rats ($n = 2$) bearing Arch and ChR2 expression in the avBST. Optrode recordings of avBST were performed both before and during laser illumination (Fig. 2). Illumination at 561-nm for 15 min suppressed the activity of Arch-expressing neurons (Fig. 2*C*). Similarly, 5-ms pulses (20 Hz for 15 min) of 473-nm light increased phasic firing rates of avBST neurons (Fig. 2*D*). Previous work found no effect of 15 min of either means of illumination on neuronal responses in avBST of rats not expressing the opsin (24), indicating that illumination alone has no effect on neural activity.

Circuit Basis for avBST Enhancement of Memory Consolidation. That avBST inhibition potentiated posttraining levels of plasma ACTH in the face of constrained CORT levels suggested a mechanism of HPA axis modulation that is more purely neuronal rather than dependent on glucocorticoid negative feedback. This raised the possibility that the memory-enhancing effect of posttraining avBST inactivation were due to disruption of its GABAergic input to (i.e., disinhibition of) HPA effector neurons in the PVH and subsequent enhancement of downstream glucocorticoid release. To investigate this, avBST neurons were transduced with the inhibitory opsin-enhanced halorhodopsin 3.0 (Halo) fused to YFP (50), and implanted optical fibers bilaterally above the PVH (Fig. 3 *A*–*C*). Immediately following IA training (0.8 mA, 1 s), half of the rats injected with Halo received

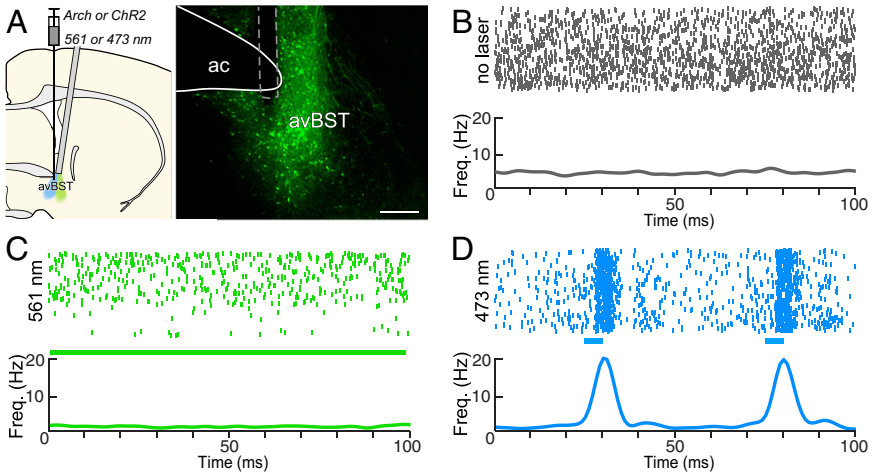

Fig. 2. Characterization of avBST neuronal activity before and during optogenetic manipulations. (*A*) Schematic diagram (*Left*) illustrating AAV injection and optrode placement during the recording during inhibition and excitation (green and blue, respectively). Epifluorescent image (*Right*) displays an implant (dashed line) for neurophysiological activity recordings made ventral to the anterior commissure (ac). (Scale bar, 300 μm.) (*B*) Raster plot (*Upper*) and summary histogram (*Lower*) of action potentials over a 15-min recording session in the absence of illumination. (*C*) Raster plot (*Upper*) of action potentials in the same neuron as in *B*, in the presence of continuous 561-nm light over a 15-min recording session. The summary histogram (*Lower*) reveals a decrease in frequency relative to baseline activity above. (*D*) Raster plot (*Upper*) of action potentials in the presence of 20-Hz pulses of 473-nm light over a 15-min recording session, and summary histogram (*Lower*), illustrating light-evoked neuronal activity. Blue bars indicate 5-ms laser pulse.

continuous illumination of avBST axons in the PVH with 561-nm light for 10 min, and the other half (i.e., control group) received no illumination.

In rats with viral injections centered in the avBST, YFP-fluorescent terminals formed a dense innervation of the PVH that ramified within the parvicellular divisions, and provided relatively sparse innervation outside of the nuclear boundary (Fig. 3*B*). Confocal laser-scanning microscopic analysis in the PVH revealed extensive colocalization of YFP-fluorescent puncta with the GABA synthetic enzyme GAD-65 (Fig. 3 *D*–*F*). In the medial parvicellular division of the PVH, these dual-labeled puncta were noted to reside in close apposition to corticotropin-releasing factor (CRF)-immunoreactive secretory neurons (Fig. 3*F*). The GABAergic signature of this pathway is consistent with the fact that the vast majority of neurons in avBST are GABAergic, with very few glutamatergic neurons (Fig. 3 *G* and *H*) (51, 52), and is similar to previous observations (24, 26, 28).

IA training significantly increased plasma ACTH and CORT levels in each group, with inhibition of avBST axons in the PVH potentiating these responses (Fig. 4 *A* and *B*). For ACTH, there were main effects of time, group, and an interaction for time and group ($F_{4,\ 92} = 20.04$, $P < 0.0001$; $F_{1,\ 23} = 6.36$, $P = 0.019$; $F_{4,\ 92} = 3.21$, $P = 0.016$; respectively). For CORT, there were main effects for time and group ($F_{4,\ 92} = 68.15$, $P < 0.001$; $F_{1,\ 23} = 6.38$, $P = 0.019$). Analysis of integrated ACTH and CORT responses revealed significant increases in the inhibition group ($t_{23} = 2.29$, $P = 0.031$; $t_{23} = 2.49$, $P = 0.020$) (Fig. 4 *A* and *B*, *Insets*). Comparisons of hormone differences at select time points after training found increased ACTH values at 10 min and 60 min ($P = 0.009$ and 0.021, respectively) and increased CORT values at 10 min and 90 min ($P = 0.009$ and 0.046) in rats receiving illumination. Consistent with the increased HPA response, illumination of avBST axons in the PVH significantly increased retention latencies when assessed 48 h later ($t_{26} = 2.14$; $P = 0.042$) (Fig. 4*C*). To verify the postsynaptic effects of avBST→PVH pathway optogenetic inhibition, rats ($n = 2$) received avBST microinjections of AAV-expressing Halo. Four weeks later, optrode recordings in the PVH were performed both before and during laser illumination in the PVH (Fig. 4*D*). Inhibiting avBST axons in the PVH reliably increased PVH spiking, indicating an inhibitory relationship between avBST and its postsynaptic target.

To determine whether the memory-impairing effects of avBST stimulation (i.e., Fig. 1*L*) also occur via this pathway, avBST neurons were transduced with ChR2 fused to YFP or with YFP alone in the control group, and optical fibers were implanted bilaterally above the PVH. Following IA training (1.0 mA, 2 s), rats received 473-nm light (20 Hz, 5-ms pulse width) to the PVH for 10 min to stimulate ChR2-transduced avBST axons, with YFP controls receiving the same illumination. Although IA training increased plasma CORT and ACTH in both groups, avBST→PVH pathway stimulation with ChR2 did not produce any differential effects (Fig. 4 *E* and *F*). Similarly, there were no differences in latencies during the 48-h retention test (Fig. 4*G*).

A Divergent Pathway from avBST Accounts for Its Memory-Attenuating Effects. Together, the results described above suggest that the memory-attenuating effects of avBST stimulation depends on a separate pathway. Recent evidence suggests that the PAG is a more central player in fear-learning circuitry than previously appreciated (35–38, 53), raising the possibility that avBST stimulation impairs retention via projections to this region.

To investigate this issue, avBST neurons were transduced with either ChR2-YFP or YFP-only and implanted optical fibers above the ventrolateral PAG (Fig. 5 *A*–*C*). Immediately following IA training (1.0 mA, 2 s), both ChR2 and YFP control rats received illumination of the axonal pathway from the avBST to PAG with 473-nm light (20 Hz, 5-ms pulse width) for 10 min. Analysis of YFP innervation of the PAG confirmed previous reports that the avBST preferentially innervates the ventrolateral subdivision, with a dearth of input to more lateral and dorsal regions (33, 34). Immunohistochemical analysis in the PAG revealed extensive colocalization of YFP-fluorescent puncta with the GABA synthetic enzyme GAD-65 (Fig. 5 *D*–*F*). IA training increased plasma CORT in both groups, with pathway stimulation producing no significant differences relative to YFP controls (Fig. 5*G*). Nevertheless, posttraining stimulation of this pathway decreased retention latencies as compared with YFP controls ($t_{20} = 2.48$; $P = 0.022$) during the 48-h retention test (Fig. 5*H*). Optrode recordings in the PAG were performed to verify the postsynaptic effects of avBST→PAG pathway stimulation using the same stimulation parameters as above. Rats ($n = 2$) received microinjections of AAV expressing ChR2 and, 4 wk later, received

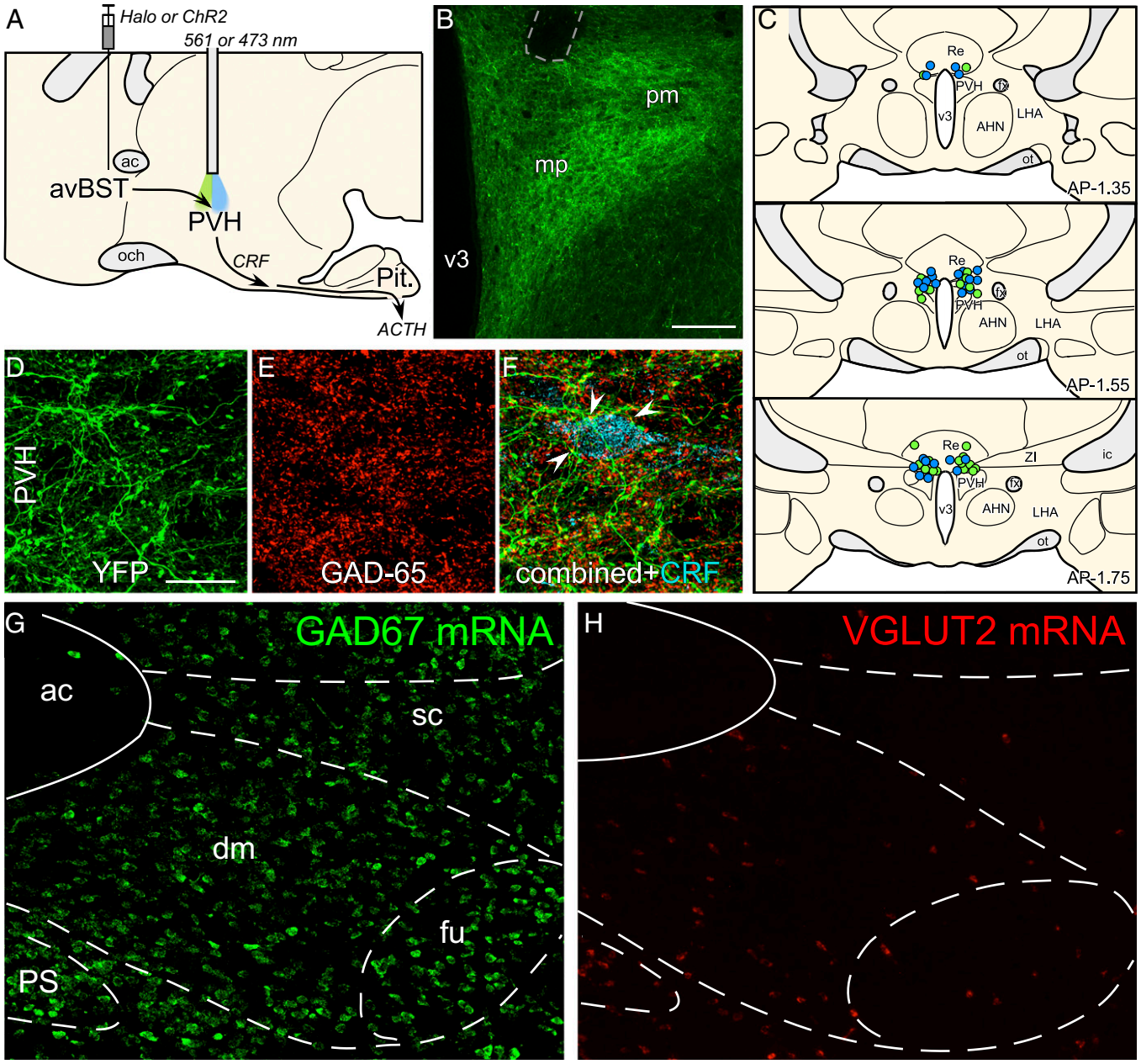

Fig. 3. Role of avBST–GABAergic input to PVH in the enhancement of memory consolidation. (*A*) Midsagittal diagram depicting AAV5 microinjection into avBST and fiber optic placement above the PVH to assess avBST→PVH pathway involvement in the posttraining modulation of HPA activity and consolidation of IA learning. (*B*) Fluorescent image illustrating the distribution of YFP-labeled terminal fields in PVH following injection in the avBST. Fiber optic implant is shown by dashed gray outline in the upper left. (Scale bar, 200 μm.) (*C*) Examples of fiber optic implants targeted toward the region immediately dorsal to the PVH for illumination. Different colored circles represent rats from separate experiments, first for Halo inhibition (green, $n = 15$), and next for ChR2 activation (blue, $n = 15$) of the avBST→PVH axonal pathway. (*D*) Confocal fluorescent images depict YFP immunoreactivity in the medial parvicellular subdivision of the PVH following AAV injection in avBST, and GAD-65, the 65-kDa form of GAD, a synthetic enzyme for GABA (*E*). (*F*) Composite of images in *D* and *F*, with the addition of immunolocalization of CRF (cyan). Numerous instances of YFP^{+}/GAD^{+} puncta were noted to make appositions with CRF-labeled neurons (arrowheads). (*G* and *H*) Fluorescent images showing in situ hybridization of GAD67 (*G*) and VGLUT2 (*H*) mRNA in avBST and its vicinity. ac, anterior commissure; AHA, anterior hypothalamic area; dm, avBST dorsomedial subdivision; fu, avBST fusiform subdivision; LHA, lateral hypothalamic area; mp, PVH medial parvicellular subdivision; och, optic chiasm; ot, optic tract; Pit., pituitary gland; pm, PVH posterior magnocellular subdivision; PS, parastrial nucleus; Re, nucleus reunions; sc, avBST subcommissural subdivision; v3, third ventricle. (Scale bar in *D*: 20 μm when applied to *D*–*F*; 100 μm when applied to *G* and *H*.)

20-Hz pulses (5 ms width) of 473-nm light in the PAG. Stimulating avBST axons in the PAG transiently decreased neuronal responses (Fig. 5*I*), indicating that there may be an inhibitory relationship between the avBST and PAG.

A final experiment examined whether the memory-enhancing effects observed following avBST inhibition could also occur through the pathway involving the ventrolateral PAG. avBST neurons were again transduced with Halo fused to YFP or with YFP alone in the control group. Following IA training (0.8 mA, 1 s), rats received continuous 561-nm light to the ventrolateral PAG for 10 min to inhibit Halo-transduced avBST axons, with YFP controls receiving the same illumination. Posttraining inhibition of this pathway did not alter adrenocortical output on the day of training (Fig. 5*J*) and did not alter retention 48-h thereafter (Fig. 5*K*).

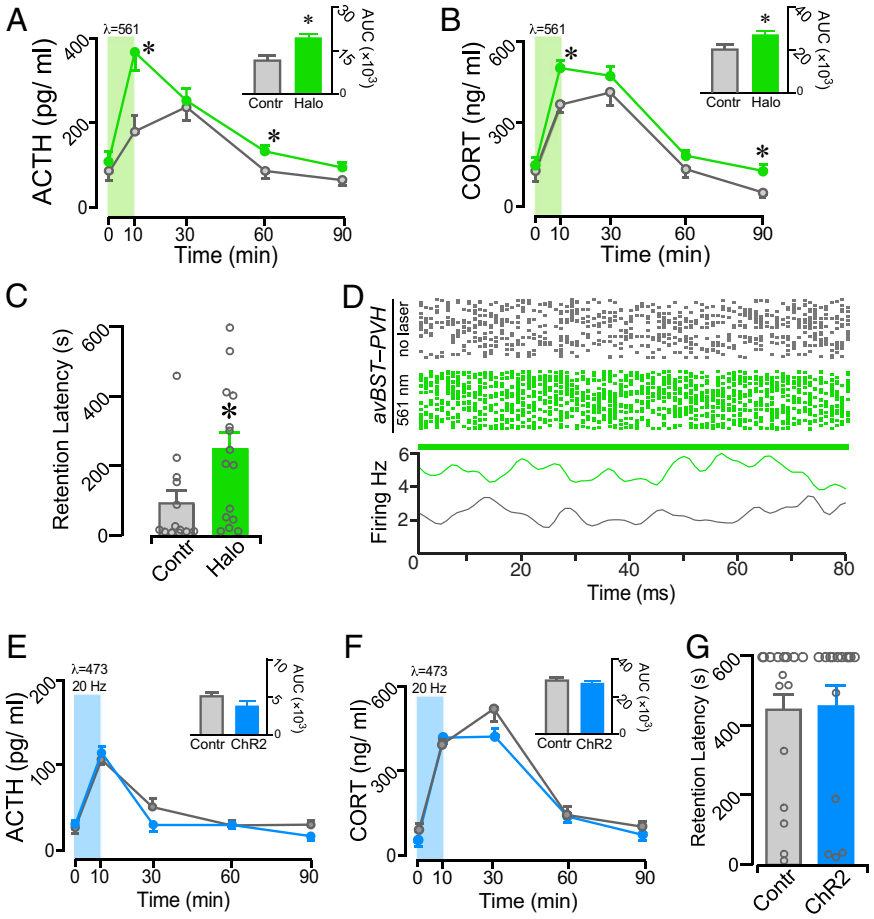

Fig. 4. Functional evidence that avBST→PVH pathway inactivation enhances memory consolidation. (*A* and *B*) Mean ± SEM of plasma ACTH (*A*) and CORT (*B*) in no-laser control and laser Halo groups before (0 min) and at various intervals following IA training. Both hormones are significantly increased in the Halo group at various intervals following illumination. (*A* and *B*, *Inset*) Integrated ACTH and CORT responses (AUC) were also significantly increased in the Halo versus control groups. (*C*) Posttraining inhibition of avBST neurons enhanced retention when measured 48 h later. (*D*) Raster plots (*Upper*) of action potentials over a 15-min recording session in the absence (gray) and presence (green) of 561-nm illumination. The summary histogram (*Lower*) reveals an increase in frequency relative to baseline activity above. (*E*–*G*) avBST→PVH pathway stimulation with ChR2 failed to alter posttraining levels of plasma ACTH (*E*) and CORT (*F*), or retention latencies (*G*) when assessed 48 h later. *$P < 0.05$.

Discussion

The present findings indicate that the avBST bidirectionally modulates consolidation of IA memory via divergent neural pathways. Optogenetic avBST inhibition for 10 min after IA training increased pituitary–adrenal responses during the posttraining period, as measured by CORT and ACTH, and enhanced retention when tested 2 d later. Pretreatment with a glucocorticoid synthesis inhibitor blocked the memory enhancement and CORT increase without altering the ACTH response, indicating that this memory-modulatory effect was mediated, at least in part, via HPA activation. However, posttraining avBST stimulation decreased retention without altering HPA output. Subsequent experiments then targeted the avBST inputs to the PVH and PAG. Posttraining inhibition of the avBST→PVH pathway mimicked the effects of avBST inhibition alone, increasing HPA output and enhancing retention, with stimulation of this pathway producing no effects. In contrast, stimulation of the avBST→PAG pathway attenuated retention without altering HPA output, with inhibition of this pathway producing no effects. Together, these results reveal a role for the avBST in modulating memory consolidation through distinct pathways using HPA-dependent and -independent mechanisms, respectively.

Glucocorticoids, avBST, and PVH. A substantial body of work indicates that systemic glucocorticoid administration enhances memory consolidation for many different forms of learning in rodents, including contextual and auditory fear conditioning (54–58), spatial and novel-object recognition (43, 59–61), and inhibitory avoidance (49, 62). Similarly, in humans, oral administration of cortisol and increased cortisol secretion induced by cold-pressor stress enhance memory consolidation for emotionally arousing stimuli (63, 64). Prior work indicates that the memory-modulatory capability of peripheral stress hormones depends, in part, on activity in the BLA. Following emotionally arousing events, glucocorticoids enhance neuronal excitability in the BLA and memory consolidation (65). Electrophysiological recordings of the BLA following IA training reveal time-dependent increases in neuronal activity that crest with plasma glucocorticoid concentrations, at around 30 min following footshock (66). The ability of the BLA to influence memory consolidation, in turn, depends on concurrent activity in other brain structures, including the BST (16, 17, 47, 67, 68). Such work appears to position the BST as downstream from the BLA in memory modulation.

Earlier work investigating the role of BST in learning regarded it as having a singular function and focused exclusively on dorsal aspects of this structure. More recently, heterogeneity in BST functions have been parcellated relative to dorsal (69), posterior (70), and ventral (24, 71) regions, and these may be further distinguished by distinct neurochemically defined subpopulations within and spanning across these regions

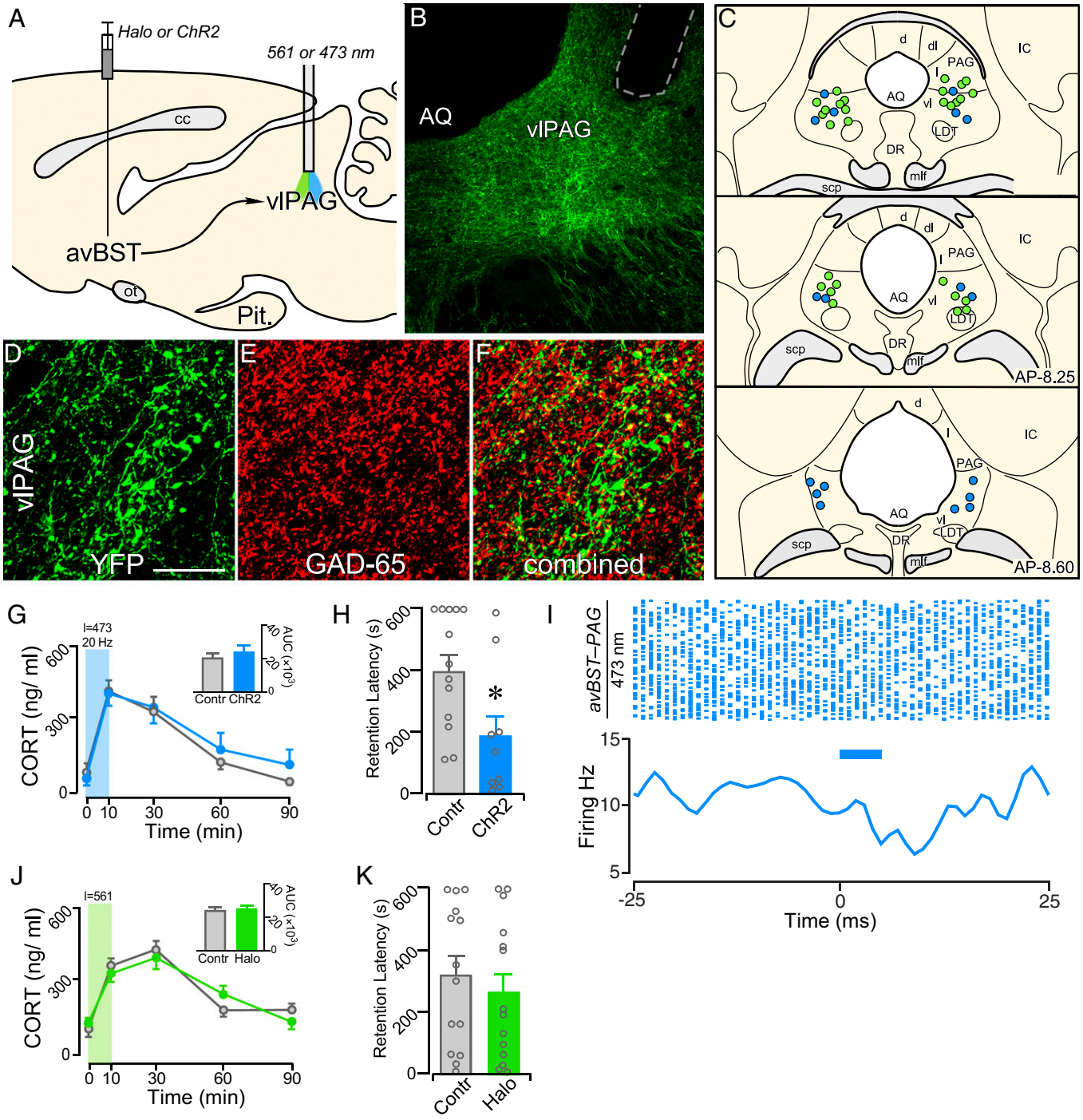

Fig. 5. Circuit basis for avBST attenuation of memory consolidation. (*A*) Midsagittal diagram depicting AAV5 microinjection into avBST and fiber optic placement above the PAG. (*B*) Fluorescent image illustrating the distribution of YFP-labeled terminal fields in ventrolateral PAG (vlPAG) following injection in the avBST. Fiber optic implant is shown by dashed gray outline. (*C*) Examples of fiber optic implants targeted toward the region immediately dorsal to the ventrolateral PAG for illumination. Different colored circles represent rats from separate experiments, first for stimulation with ChR2 (blue, $n = 9$) and next for inhibition with Halo (green, $n = 14$) of the avBST→ventrolateral PAG axonal pathway. (*D*–*F*) Confocal fluorescent images show YFP immunoreactivity in the ventrolateral PAG following AAV injection in avBST (*D*), GAD-65 immunofluoresence (*E*), and a composite of these images (*F*) illustrating instances of YFP^{+}/GAD^{+} colocalization. (Scale bar in *D*: 250 μm when applied to *B*; 20 μm when applied to *D*–*F*.) (*G*) Mean ± SEM of plasma CORT in YFP and ChR2 groups before (0 min) and at various intervals following IA training. (*G*, *Inset*) Integrated CORT responses (AUC). (*H*) Posttraining stimulation of the avBST→ventrolateral PAG pathway with ChR2 attenuated retention latencies, when measured 48 h later. (*I*) Raster plot (*Upper*) of action potentials in the presence of 20-Hz pulses of 473-nm light over a 15-min recording session, and summary histogram (*Lower*), illustrating light-evoked neuronal activity. Blue bars indicate 5-ms laser pulse. (*J* and *K*) avBST→ PVH pathway inhibition with Halo failed to alter either posttraining levels of plasma CORT (*I*), or retention latencies (*J*) when assessed 48 h later. *$P < 0.05$. AQ, Sylvian aqueduct; cc, corpus callosum; d, PAG dorsal subdivision; dl, PAG dorsolateral subdivision; DR, dorsal raphe nucleus; IC, inferior colliculus; l, PAG lateral subdivision; LDT; laterodorsal tegmental nucleus; mlf, medial longitudinal fasiculus; Pit., pituitary gland; scp, superior cerebellar peduncle; vl, PAG ventrolateral subdivision.

(52, 72–74). The present study targeted the avBST region, as opposed to the dorsal BST, because evidence suggests that the avBST is capable of potently modulating adaptive responses to stressors, particularly HPA axis activity (25–28, 31, 75, 76). This suggested the possibility that avBST could influence memory consolidation as an upstream regulator of stress responses.

Indeed, the first central finding of the present study reveals a role for the avBST in regulating memory consolidation. In particular, the results indicate that avBST activity alters consolidation via the regulation of glucocorticoid secretion through its GABAergic input to the HPA effector region of the PVH. This suggests that, in contrast to studies on the dorsal aspects of the BST, the avBST acts upstream from BLA-dependent processes by regulating glucocorticoid secretion. Interestingly, inhibition, but not stimulation, of the avBST→PVH pathway altered memory consolidation and HPA output. Thus, the present findings suggest that activity of this circuit is necessary, but not sufficient, to restrain the extent of HPA output following an aversive experience which, in turn, reduces the strength of the resulting memory of the experience. Along these lines, diminished activity in this pathway may provide an endogenous mechanism for augmenting HPA output and memory consolidation following an emotionally arousing event.

As each major BST subdivision expresses the type II glucocorticoid receptor (77–79), this raises the possibility that HPA axis activation influences the avBST and its modulation of memory consolidation. However, the present results indicate that posttraining avBST inhibition was accompanied by increases in plasma ACTH even when metyrapone administration prevented the footshock-induced increase in CORT, suggesting that the ability of avBST to regulate the HPA axis involves some degree of independence from feedback influences of CORT (Fig. 1*G*) (e.g., see ref. 80). This supports the idea that the memory-modulatory influences of the avBST occur via a circuit-based mechanism involving the PVH rather than via glucocorticoid feedback. Nevertheless, the possible involvement of BST-glucocorticoid receptor effects on memory consolidation at later times after training warrants consideration in future studies.

avBST and PAG. The second central finding from the present study is that avBST inputs to the ventrolateral PAG also influence memory consolidation and do so in a manner independent of HPA axis modulation. These results build on recent evidence implicating the PAG more directly in learning than previously appreciated (35, 38, 81), although the precise role of the PAG in aversive learning is still not clear. Whereas past studies suggest that the ventrolateral PAG is involved in the expression of conditioned freezing responses and defensive behaviors (82, 83), there is also a growing appreciation for the role of the ventrolateral PAG in the acquisition of fear conditioning. A current perspective is that the ventrolateral PAG relays aversive instructive signals, presumably to other brain regions (e.g., the BLA during auditory Pavlovian fear conditioning) to enable learning-related plasticity (81). This view is based upon evidence that ventrolateral PAG modifies aversive stimuli-evoked activity in the BLA (38), whereas chemogenetic, optogenetic, and pharmacological manipulations of the ventrolateral PAG disrupt acquisition of conditioned fear (35, 37, 38, 53, 81, 84). Another recent study found that enhanced activity in the ventrolateral PAG reflects an increased probability of threat onset (e.g., footshock) (35). As the present results found that stimulation of GABAergic avBST inputs to the ventrolateral PAG impaired retention, this raises the possibility that such activity disrupts the ability of the PAG to convey this instructive signal as part of a memory consolidation process and warrants more careful consideration of this novel circuit for future studies. However, inhibition of this pathway did not alter consolidation, suggesting a lack of activity in this pathway at least in the present experimental circumstances.

One outstanding question concerns the temporal sequence for how the avBST→ventrolateral PAG pathway modulates memory consolidation. As the present study involved manipulations of the avBST→ventrolateral PAG pathway after IA training, this more directly implicates the ventrolateral PAG in memory consolidation that is neither directly connected with acquisition or expression and points to the avBST as an important upstream modulatory influence. Indeed, it appears that the same circuits and structures (e.g., the PAG) that generate defensive behaviors and stress-adaptive responses are also important after an aversive event for influencing memory consolidation.

Nonetheless, the present findings support the ability of avBST activity to modulate memory consolidation in a bidirectional manner. Although activity in this structure appears to be both necessary and sufficient for enhancing and attenuating retention, respectively, a surprising finding was that each effect depended on distinct pathways involving the PVH and the ventrolateral PAG, respectively. Recent evidence implicates these pathways in the modulation of endocrine and behavioral stress-adaptive behaviors (23, 24), whereas diminished activity may account for some of the endocrine and behavioral disturbances that are common in stress-related psychiatric disorders. The fact that all manipulations in the present study were given during the posttraining period enables the distinction between the role of the circuits in adapting to exposure to the stressor and their role in altering mnemonic processes following an aversive learning event. Nevertheless, additional work is needed to assess whether the avBST and related circuitry have distinct roles in stress adaptation and memory modulation under naturalistic conditions. Considering the persistence or oversaliency of memories that occurs in a variety of stress-related pathologies, such as posttraumatic stress disorder, avBST dysfunction may provide a novel mechanism connecting stress susceptibility to the mnemonic components of stress-based disorders.

Materials and Methods

Animals and Treatments. Adult male Sprague-Dawley rats (225 to 250 g at time of arrival; Charles River Laboratories) were used. Animals were maintained on a 12:12 light/dark cycle (lights on at 0600 hours) in an Association for Assessment and Accreditation of Laboratory Animal Care-approved vivarium with ad libitum access to food and water. Rats were acclimated to the vivarium housing conditions for 7 d prior to surgery. All procedures were in accord with the National Institutes of Health's *Guide for the Care and Use of Laboratory Animals* (85) and were approved by the University of Iowa Institutional Animal Care and Use Committee.

Surgeries. Rats were anesthetized with 4% isoflurane in oxygen, placed in a stereotaxic frame (Kopf Instruments), and received a presurgical analgesic (2 mg/kg meloxicam, subcutaneously). Surgical anesthesia was maintained with 1.5 to 2% isoflurane. A midline incision was made down the scalp and a craniotomy was performed above the region of interest. Rats received bilateral microinjections (350 nL per side) of virus solution directed at avBST (anteroposterior, AP: −0.10 mm relative to bregma; mediolateral, ML: ±1.20 mm; dorsoventral, DV: −7.45 mm). The virus solution contained AAV5 coding either eArch3.0-eYFP, eNpHR3.0-eYFP, ChR2(E123A)-eYFP, or eYFP alone, all of which were under the control of the human synapsin-1 promoter (39, 40, 50). Optical fibers (200-μm diameter, 0.37 N.A.; Thorlabs) secured inside of steel ferrules (PlasticsOne) were implanted either immediately dorsal to avBST (AP: −0.10 mm; ML: 2.35 mm; DV: −6.60 mm; 8°), avBST terminal fields in the PVH (AP: −1.55 mm; ML: 1.65 mm; DV: −7.00 mm; 10°), or above the ventrolateral PAG (AP: −7.85 mm; ML: 1.80 mm; DV: −5.20; 10°) and then secured with dental cement and surgical screws. After 3 to 6 wk recovery, rats began the behavioral procedures.

Hormone Assays. Two days prior to IA training, rats received implants with indwelling jugular catheters (86, 87). Sealed jugular catheters (polyethylene PE 50) with a SILASTIC (Dow-Corning) tip containing sterile heparin-saline (50 U/mL) were implanted under isoflurane anesthesia. The internalized

SILASTIC tip was positioned at the atrium and was exteriorized at the interscapular region of the neck. At 0600 hours on day 1 of the experiment (i.e., a time chosen since it coincides with the onset of the diurnal trough of the circadian CORT cycle) (86), rats were brought to the procedure room and jugular catheters were connected to 1-mL syringes filled with sterile heparinized saline. Catheters were flushed with heparinized saline prior to blood collection. After 90 min of habituation and prior to the onset of behavioral training, blood samples were collected prior to IA training (0 min), and at 10, 30, 60, and 90-min intervals thereafter to monitor elevations in stress hormone levels. Upon collection, each sample was immediately placed in a chilled conical vial containing 15 μL EDTA/aprotinin, centrifuged for 20 min, and plasma was fractionated for storage at −80 °C. A two-site radioimmunoassay (MP Biomedicals) incorporating rabbit antisera raised against ACTH-BSA with ^{125}I-ACTH-BSA serving as a tracer was used for measurement of plasma ACTH. Intraassay and interassay coefficients of variation for ACTH radioimmunoassay were 3% and 7%, respectively. Similarly, plasma CORT was measured without extraction using rabbit antisera raised against CORT-BSA with ^{125}I-CORT-BSA serving as tracer (MP Biomedicals), with intra/inter-assay coefficients of 5% and 10%, respectively, and a sensitivity of 8 ng/mL. Catheter viability was consistently >80% across all experiments. Rats with failed catheter patency were still included in behavioral analyses.

Drug Treatment. One experiment involved systemic injections of metyrapone 90 min prior to IA training, to reversibly inhibit steroid 11β-hydroxylase in the adrenal cortex (Sigma). The dose of metyrapone (50 mg/kg, subcutaneously) was selected as based on prior knowledge of its capacity to suppress stress-induced elevations in plasma CORT, without leading to significant impairments in memory consolidation following IA training (45, 88). To reach the appropriate concentration, the drug was dissolved in 40% polyethylene glycol and diluted with 0.9% saline.

Behavioral Procedures. All rats were trained on the single-trial step-through IA task (45, 46, 89). The IA apparatus was a trough-shaped box segmented into one-third (30 cm) of an illuminated white plastic bottom and the remaining two-thirds (60 cm) darkened stainless steel. The 60-cm darkened stainless-steel portion of the apparatus was connected to a shock generator, and timer. A retractable stainless steel door separated the two compartments.

Prior to experimentation, rats were handled for 3 min daily, and habituated for 1 h to the procedure room each day for 7 d. During IA training (day 1), rats were placed in the enclosed lit compartment to allow for a brief period of acclimation (~10 s). The door was then opened to allow free exploration of the apparatus. Upon entry into the darkened compartment, the retractable door was closed to prevent the rat from returning to the lit side. When the rat reached the end of the dark compartment, it received a single inescapable footshock (1.0 mA, 2-s duration for rats transduced with ChR2 in avBST neurons; 0.8 mA, 1-s duration for experiments involving transduction with Arch and Halo; different footshock intensities were used to prevent floor and ceiling effects, respectively) (46–49). Thereafter, the rat was left in the dark compartment for 20 s and then removed for optical manipulation and further blood collection. For retention testing 48 h later, rats were placed back into the lit compartment of the IA chamber with the door retracted. Rats' latency (in seconds) to cross into the dark compartment was measured and used as the index of retention with a maximum latency of 600 s.

Optical Procedures. Surgically implanted optic ferrules were connected to an insulated optical fiber directed from a 561-nm (Laser Century), or 473-nm light source (OptoEngine). Laser output was adjusted to direct 10 mW at the tip of the implanted optical fibers, which is sufficient to activate opsins within a 0.46-mm radius of spherical illumination below the termination of the fiber optic (46, 90). In all experiments, illumination began 20 s following application of footshock and continued for 10 min. For Arch and Halo experiments, continuous 561-nm light illumination was used. Experiments involving avBST cell body inactivation were carried out using Arch, and Halo was used for pathway inactivation, as based on evidence that illumination of Arch at axon terminals over a several minute period may paradoxically increase spontaneous transmitter release (91). For ChR2 experiments, trains of 5-ms pulses at either 20 Hz or 40 Hz (Master-9 pulse generator) were used. Experiments involved the use of controls receiving the same illumination parameters as their respective experimental counterparts, unless otherwise noted.

Optrode Recordings. In a separate experiment, rats were injected with viral solutions for the transduction of Arch, Halo, or ChR2 in avBST neurons. Four weeks later, the same rats underwent an additional stereotaxic surgery for the implantation of a combined microwire array/optical fiber, or optrode (MicroProbes for Life Science), and recording of optically evoked excitation or inhibition of AAV-transduced avBST neurons or separately, postsynaptic characterization of single unit PVH and vlPAG neuronal activity following avBST terminal excitation and inhibition. Following initial induction of anesthesia, animals received an intraperitoneal injection of ketamine (100 mg/kg) and xylazine (10 mg/kg) and subsequently maintained at surgical level anesthesia with additional injections of ketamine (30 mg/kg), as necessary. The scalp was then retracted and skull leveled between bregma and lambda before commencement of craniotomy above the avBST, PVH, or ventrolateral PAG of the right hemisphere. Insertion of the ground wire was performed in a separate hole and secured to skull screws. The optrode was positioned above the avBST, PVH, or PAG and slowly lowered (0.1 mm/min) into the most dorsal aspect of each region (avBST: DV −7.2 mm; PVH: DV −7.45 mm; vlPAG: −5.2 mm relative to dura).

Using an online oscilloscope and audio monitor to identify single neurons, neuronal recordings were made using a multielectrode recording system (Plexon). Recordings were made with the following parameters: avBST neuron recording experiments: 0 to 15 min, laser off; 15 to 30 min, either 473-nm laser pulsed at 20 Hz with 10% duty cycle, or 561 nm laser on; 30 to 45 min, laser off. PVH neuron recording experiments: 0 to 5 min, laser off; 5 to 10 min (20-s laser off – 20-s laser on – 20-s laser off); 10 to 20 min laser on; 20 to 21 min, laser off. Ventrolateral PAG neuron recording experiments: 0 to 1 min, laser off; 1 to 2 min 1 Hz to 20 Hz ramping 473-nm laser on with 10% duty cycle; 2 to 5 min 473-nm laser pulsed at 20 Hz with 10% duty cycle. After the initial recording, the optrode was lowered in 0.15-mm increments for a total of four recordings. After the recording session, the hardware was removed and animals were prepared for histology (see below). To analyze signals offline and for the removal artifacts, the Plexon Off-line Sorter program was used. All cells that fired at rates >0.1 Hz were analyzed. Principle component analysis (PCA) and waveform shape were used for spike sorting. All single units exhibited: 1) Consistent waveform shape, 2) separable clusters in PCA space, 3) average amplitude >three times background activity, and 4) refractory periods of <2 ms. Custom MATLAB routines were used to analyze neuronal activity.

Histology and Tissue Processing. Rats were anesthetized with pentobarbital (Fatal Plus; 100 mg/kg, i.p.) and transcardially perfused at a rate of 55 mL/min with 100 mL of 0.9% NaCl, followed by 900 mL of ice-chilled 4% paraformaldehyde (PFA). Brains were then dissected and postfixed in 4% PFA at 4 °C for 4 h prior to transfer into a 20% sucrose/potassium phosphate buffer cryoprotectant for overnight storage. Coronal sections (30 μm) were collected in a 1:5 series on a sliding microtome (Leica). In all cases, sections were stored in a cryoprotectant solution at −20 °C. Verification of viral expression, and placement of optical probes was performed by visualization of YFP expression under epifluorescence with a compound light microscope (Leica), and confirmed based on the cytoarchitectonic characteristics for the structures of interest (92, 93). Rats with incorrect placement of virus or optic probes were excluded from subsequent analyses.

Hybridization Histochemistry. In situ hybridization was performed using antisense oligonucleotide probes from RNAscope (Advanced Cell Diagnostics) (94–96). This variation of in situ hybridization utilizes DNA *z*-blocks containing complimentary 18- to 25-bp target RNA sequences, a spacer sequence, and a 14-base oligonucleotide tail that allows single-cell resolution of targeted mRNA with a high degree of specificity. Probes targeting GAD1 (ACDBio catalog #316401), vGlut2 (ACDBio catalog #317011), and CRF (ACDBio catalog #318931) were obtained and hybridization was performed using RNAscope Fluorescent Multiplex v2 (Advanced Cell Diagnostics). Visualization was performed using fluorophores (Fluorescein, Cyanine 3, Cyanine 5) with fluorescent signal enhancement using a modified tyramide signal amplification method (Perkin-Elmer). Slides were counterstained with DAPI (Thermo Fisher) and coverslipped with ProLong Gold antifade reagent.

Immunohistochemistry. Localization of antigens were performed on free-floating sections. Primary antisera raised against anti-GFP (rabbit polyclonal; Thermo Fisher) and GAD-65 (mouse monoclonal; University of Iowa Developmental Studies Hybridoma Bank) were visualized respectively with goat anti-rabbit (Alexa 488; Thermo Fisher) or goat anti-mouse (Alexa 568; Thermo Fisher). CRF was immunolocalized using an antiserum raised against rat CRF (rC68, rabbit polyclonal; Paul Sawchenko, The Salk Institute of Biological Studies, La Jolla, CA), followed by incubation with biotinylated goat anti-rabbit IgG and streptavidin-conjugated Alexa 633 (Thermo Fisher).

Statistics. Plasma levels of stress hormones were analyzed using a repeated measures two-way ANOVA with blood collection time point (0, 10, 30, 60, 90

min) as the within-subjects variable, and optogenetic treatment as the between-subjects factor. Post hoc pairwise comparisons using Fisher's least significant difference were used when appropriate (i.e., $P < 0.05$). All main analyses were considered significant at $P < 0.05$. Integrated hormone levels (i.e., AUC), and retention latency data were analyzed using an unpaired *t* test. Data are expressed as mean ± SEM.

Data Availability. The data presented in this report are available in Datasets S1–S4.

ACKNOWLEDGMENTS. This work was supported by National Institutes of Health R01 MH-119106, R56 MH-095972, and National Alliance for Research on Schizophrenia and Depression Independent Investigator grants.

1. J. L. McGaugh, *Memory and Emotion: The Making of Lasting Memories* (Columbia University Press, New York, 2003).
2. J. L. McGaugh, Making lasting memories: Remembering the significant. *Proc. Natl. Acad. Sci. U.S.A.* **110** (suppl. 2), 10402–10407 (2013).
3. J. L. McGaugh, Memory—A century of consolidation. *Science* **287**, 248–251 (2000).
4. P. E. Gold, R. van Buskirk, Posttraining brain norepinephrine concentrations: Correlation with retention performance of avoidance training and with peripheral epinephrine modulation of memory processing. *Behav. Biol.* **23**, 509–520 (1978).
5. P. E. Gold, R. B. Van Buskirk, Facilitation of time-dependent memory processes with posttrial epinephrine injections. *Behav. Biol.* **13**, 145–153 (1975).
6. C. Sandi, M. T. Pinelo-Nava, Stress and memory: Behavioral effects and neurobiological mechanisms. *Neural Plast.* **2007**, 78970 (2007).
7. B. Roozendaal, B. S. McEwen, S. Chattarji, Stress, memory and the amygdala. *Nat. Rev. Neurosci.* **10**, 423–433 (2009).
8. J. L. McGaugh, B. Roozendaal, Role of adrenal stress hormones in forming lasting memories in the brain. *Curr. Opin. Neurobiol.* **12**, 205–210 (2002).
9. E. R. de Kloet, M. S. Oitzl, M. Joëls, Stress and cognition: Are corticosteroids good or bad guys? *Trends Neurosci.* **22**, 422–426 (1999).
10. K. C. Liang, R. G. Juler, J. L. McGaugh, Modulating effects of posttraining epinephrine on memory: Involvement of the amygdala noradrenergic system. *Brain Res.* **368**, 125–133 (1986).
11. G. L. Quirarte, B. Roozendaal, J. L. McGaugh, Glucocorticoid enhancement of memory storage involves noradrenergic activation in the basolateral amygdala. *Proc. Natl. Acad. Sci. U.S.A.* **94**, 14048–14053 (1997).
12. B. Ferry, B. Roozendaal, J. L. McGaugh, Role of norepinephrine in mediating stress hormone regulation of long-term memory storage: A critical involvement of the amygdala. *Biol. Psychiatry* **46**, 1140–1152 (1999).
13. B. Roozendaal, J. L. McGaugh, Amygdaloid nuclei lesions differentially affect glucocorticoid-induced memory enhancement in an inhibitory avoidance task. *Neurobiol. Learn. Mem.* **65**, 1–8 (1996).
14. B. Roozendaal *et al*., Basolateral amygdala noradrenergic activity mediates corticosterone-induced enhancement of auditory fear conditioning. *Neurobiol. Learn. Mem.* **86**, 249–255 (2006).
15. K. C. Liang, J. L. McGaugh, Lesions of the stria terminalis attenuate the amnestic effect of amygdaloid stimulation on avoidance responses. *Brain Res.* **274**, 309–318 (1983).
16. K. C. Liang, J. L. McGaugh, Lesions of the stria terminalis attenuate the enhancing effect of post-training epinephrine on retention of an inhibitory avoidance response. *Behav. Brain Res.* **9**, 49–58 (1983).
17. K. C. Liang, H. C. Chen, D. Y. Chen, Posttraining infusion of norepinephrine and corticotropin releasing factor into the bed nucleus of the stria terminalis enhanced retention in an inhibitory avoidance task. *Chin. J. Physiol.* **44**, 33–43 (2001).
18. M. A. Lebow, A. Chen, Overshadowed by the amygdala: The bed nucleus of the stria terminalis emerges as key to psychiatric disorders. *Mol. Psychiatry* **21**, 450–463 (2016).
19. N. Z. Gungor, D. Paré, Functional heterogeneity in the bed nucleus of the stria terminalis. *J. Neurosci.* **36**, 8038–8049 (2016).
20. S. E. Daniel, D. G. Rainnie, Stress modulation of opposing circuits in the bed nucleus of the stria terminalis. *Neuropsychopharmacology* **41**, 103–125 (2016).
21. O. E. Rodríguez-Sierra, H. K. Turesson, D. Pare, Contrasting distribution of physiological cell types in different regions of the bed nucleus of the stria terminalis. *J. Neurophysiol.* **110**, 2037–2049 (2013).
22. C. C. Crestani *et al*., Mechanisms in the bed nucleus of the stria terminalis involved in control of autonomic and neuroendocrine functions: A review. *Curr. Neuropharmacol.* **11**, 141–159 (2013).
23. J. J. Radley, S. B. Johnson, Anteroventral bed nuclei of the stria terminalis neurocircuitry: Towards an integration of HPA axis modulation with coping behaviors—Curt Richter Award Paper 2017. *Psychoneuroendocrinology* **89**, 239–249 (2018).
24. S. B. Johnson *et al*., A basal forebrain site coordinates the modulation of endocrine and behavioral stress responses via divergent neural pathways. *J. Neurosci.* **36**, 8687–8699 (2016).
25. D. C. Choi *et al*., Bed nucleus of the stria terminalis subregions differentially regulate hypothalamic-pituitary-adrenal axis activity: Implications for the integration of limbic inputs. *J. Neurosci.* **27**, 2025–2034 (2007).
26. W. E. Cullinan, J. P. Herman, S. J. Watson, Ventral subicular interaction with the hypothalamic paraventricular nucleus: Evidence for a relay in the bed nucleus of the stria terminalis. *J. Comp. Neurol.* **332**, 1–20 (1993).
27. J. J. Radley, P. E. Sawchenko, A common substrate for prefrontal and hippocampal inhibition of the neuroendocrine stress response. *J. Neurosci.* **31**, 9683–9695 (2011).
28. J. J. Radley, K. L. Gosselink, P. E. Sawchenko, A discrete GABAergic relay mediates medial prefrontal cortical inhibition of the neuroendocrine stress response. *J. Neurosci.* **29**, 7330–7340 (2009).
29. J. D. Dunn, Plasma corticosterone responses to electrical stimulation of the bed nucleus of the stria terminalis. *Brain Res.* **407**, 327–331 (1987).
30. S. B. Johnson *et al*., Prefrontal-bed nucleus circuit modulation of a passive coping response set. *J. Neurosci.* **39**, 1405–1419 (2019).
31. D. C. Choi *et al*., The anteroventral bed nucleus of the stria terminalis differentially regulates hypothalamic-pituitary-adrenocortical axis responses to acute and chronic stress. *Endocrinology* **149**, 818–826 (2008).
32. P. L. W. Colmers, J. S. Bains, Presynaptic mGluRs control the duration of endocannabinoid-mediated DSI. *J. Neurosci.* **38**, 10444–10453 (2018).
33. H. W. Dong, G. D. Petrovich, A. G. Watts, L. W. Swanson, Basic organization of projections from the oval and fusiform nuclei of the bed nuclei of the stria terminalis in adult rat brain. *J. Comp. Neurol.* **436**, 430–455 (2001).
34. H. W. Dong, L. W. Swanson, Projections from bed nuclei of the stria terminalis, dorsomedial nucleus: Implications for cerebral hemisphere integration of neuroendocrine, autonomic, and drinking responses. *J. Comp. Neurol.* **494**, 75–107 (2006).
35. K. M. Wright, M. A. McDannald, Ventrolateral periaqueductal gray neurons prioritize threat probability over fear output. *eLife* **8**, e45013 (2019).
36. S. Cole, G. P. McNally, Complementary roles for amygdala and periaqueductal gray in temporal-difference fear learning. *Learn. Mem.* **16**, 1–7 (2008).
37. C. Arico, E. E. Bagley, P. Carrive, N. Assareh, G. P. McNally, Effects of chemogenetic excitation or inhibition of the ventrolateral periaqueductal gray on the acquisition and extinction of Pavlovian fear conditioning. *Neurobiol. Learn. Mem.* **144**, 186–197 (2017).
38. J. P. Johansen, J. W. Tarpley, J. E. LeDoux, H. T. Blair, Neural substrates for expectation-modulated fear learning in the amygdala and periaqueductal gray. *Nat. Neurosci.* **13**, 979–986 (2010).
39. E. S. Boyden, F. Zhang, E. Bamberg, G. Nagel, K. Deisseroth, Millisecond-timescale, genetically targeted optical control of neural activity. *Nat. Neurosci.* **8**, 1263–1268 (2005).
40. B. Y. Chow *et al*., High-performance genetically targetable optical neural silencing by light-driven proton pumps. *Nature* **463**, 98–102 (2010).
41. G. F. Alheid, L. Heimer, New perspectives in basal forebrain organization of special relevance for neuropsychiatric disorders: The striatopallidal, amygdaloid, and corticopetal components of substantia innominata. *Neuroscience* **27**, 1–39 (1988).
42. J. S. de Olmos, C. A. Beltamino, G. F. Alheid, "Amygdala and extended amygdala of the rat a cytoarchitectonical, fibroarchitectonical, and chemoarchitectonical survey" in *The Rat Nervous System*, G. Paxinos, Ed. (Academic Press, Sydney, 2004), pp. 495–578.
43. B. Roozendaal, G. Portillo-Marquez, J. L. McGaugh, Basolateral amygdala lesions block glucocorticoid-induced modulation of memory for spatial learning. *Behav. Neurosci.* **110**, 1074–1083 (1996).
44. B. Roozendaal, J. L. McGaugh, The memory-modulatory effects of glucocorticoids depend on an intact stria terminalis. *Brain Res.* **709**, 243–250 (1996).
45. B. Roozendaal, O. Carmi, J. L. McGaugh, Adrenocortical suppression blocks the memory-enhancing effects of amphetamine and epinephrine. *Proc. Natl. Acad. Sci. U.S.A.* **93**, 1429–1433 (1996).
46. M. L. Huff, R. L. Miller, K. Deisseroth, D. E. Moorman, R. T. LaLumiere, Posttraining optogenetic manipulations of basolateral amygdala activity modulate consolidation of inhibitory avoidance memory in rats. *Proc. Natl. Acad. Sci. U.S.A.* **110**, 3597–3602 (2013).
47. T. L. Liu, D. Y. Chen, K. C. Liang, Post-training infusion of glutamate into the bed nucleus of the stria terminalis enhanced inhibitory avoidance memory: An effect involving norepinephrine. *Neurobiol. Learn. Mem.* **91**, 456–465 (2009).
48. D. Y. Chen, D. Bambah-Mukku, G. Pollonini, C. M. Alberini, Glucocorticoid receptors recruit the CaMKIIα-BDNF-CREB pathways to mediate memory consolidation. *Nat. Neurosci.* **15**, 1707–1714 (2012).
49. B. Roozendaal, C. L. Williams, J. L. McGaugh, Glucocorticoid receptor activation in the rat nucleus of the solitary tract facilitates memory consolidation: Involvement of the basolateral amygdala. *Eur. J. Neurosci.* **11**, 1317–1323 (1999).
50. X. Han, E. S. Boyden, Multiple-color optical activation, silencing, and desynchronization of neural activity, with single-spike temporal resolution. *PLoS One* **2**, e299 (2007).
51. T. Kudo *et al*., Three types of neurochemical projection from the bed nucleus of the stria terminalis to the ventral tegmental area in adult mice. *J. Neurosci.* **32**, 18035–18046 (2012).
52. W. J. Giardino *et al*., Parallel circuits from the bed nuclei of stria terminalis to the lateral hypothalamus drive opposing emotional states. *Nat. Neurosci.* **21**, 1084–1095 (2018).
53. N. Assareh, E. E. Bagley, P. Carrive, G. P. McNally, Brief optogenetic inhibition of rat lateral or ventrolateral periaqueductal gray augments the acquisition of Pavlovian fear conditioning. *Behav. Neurosci.* **131**, 454–459 (2017).
54. A. C. Medina *et al*., Glucocorticoid administration into the dorsal striatum [corrected] facilitates memory consolidation of inhibitory avoidance training but not of the context or footshock components. *Learn. Mem.* **14**, 673–677 (2007). Erratum in *Learn. Mem.* **14**, 703 (2007).
55. N. Kaouane *et al*., Glucocorticoids can induce PTSD-like memory impairments in mice. *Science* **335**, 1510–1513 (2012).
56. G. K. Hui *et al*., Memory enhancement of classical fear conditioning by post-training injections of corticosterone in rats. *Neurobiol. Learn. Mem.* **81**, 67–74 (2004).

57. M. I. Cordero, J. J. Merino, C. Sandi, Correlational relationship between shock intensity and corticosterone secretion on the establishment and subsequent expression of contextual fear conditioning. *Behav. Neurosci.* **112**, 885–891 (1998).
58. M. I. Cordero, C. Sandi, A role for brain glucocorticoid receptors in contextual fear conditioning: Dependence upon training intensity. *Brain Res.* **786**, 11–17 (1998).
59. B. Roozendaal, Q. K. Griffith, J. Buranday, D. J. De Quervain, J. L. McGaugh, The hippocampus mediates glucocorticoid-induced impairment of spatial memory retrieval: Dependence on the basolateral amygdala. *Proc. Natl. Acad. Sci. U.S.A.* **100**, 1328–1333 (2003).
60. S. Okuda, B. Roozendaal, J. L. McGaugh, Glucocorticoid effects on object recognition memory require training-associated emotional arousal. *Proc. Natl. Acad. Sci. U.S.A.* **101**, 853–858 (2004).
61. C. Sandi, M. Loscertales, C. Guaza, Experience-dependent facilitating effect of corticosterone on spatial memory formation in the water maze. *Eur. J. Neurosci.* **9**, 637–642 (1997).
62. C. Sandi, S. P. Rose, Corticosterone enhances long-term retention in one-day-old chicks trained in a weak passive avoidance learning paradigm. *Brain Res.* **647**, 106–112 (1994).
63. T. W. Buchanan, W. R. Lovallo, Enhanced memory for emotional material following stress-level cortisol treatment in humans. *Psychoneuroendocrinology* **26**, 307–317 (2001).
64. L. Cahill, L. Gorski, K. Le, Enhanced human memory consolidation with post-learning stress: Interaction with the degree of arousal at encoding. *Learn. Mem.* **10**, 270–274 (2003).
65. S. Duvarci, D. Paré, Glucocorticoids enhance the excitability of principal basolateral amygdala neurons. *J. Neurosci.* **27**, 4482–4491 (2007).
66. J. G. Pelletier, E. Likhtik, M. Filali, D. Paré, Lasting increases in basolateral amygdala activity after emotional arousal: Implications for facilitated consolidation of emotional memories. *Learn. Mem.* **12**, 96–102 (2005).
67. J. L. McGaugh, C. K. McIntyre, A. E. Power, Amygdala modulation of memory consolidation: Interaction with other brain systems. *Neurobiol. Learn. Mem.* **78**, 539–552 (2002).
68. R. T. LaLumiere, J. L. McGaugh, C. K. McIntyre, Emotional modulation of learning and memory: Pharmacological implications. *Pharmacol. Rev.* **69**, 236–255 (2017).
69. S. Y. Kim *et al*., Diverging neural pathways assemble a behavioural state from separable features in anxiety. *Nature* **496**, 219–223 (2013).
70. M. J. Henckens *et al*., CRF receptor type 2 neurons in the posterior bed nucleus of the stria terminalis critically contribute to stress recovery. *Mol. Psychiatry* **22**, 1691–1700 (2017).
71. J. H. Jennings *et al*., Distinct extended amygdala circuits for divergent motivational states. *Nature* **496**, 224–228 (2013).
72. T. L. Fetterly *et al*., α_{2A}-Adrenergic receptor activation decreases parabrachial nucleus excitatory drive onto BNST CRF neurons and reduces their activity in vivo. *J. Neurosci.* **39**, 472–484 (2019).
73. M. B. Pomrenze, T. L. Fetterly, D. G. Winder, R. O. Messing, The corticotropin releasing factor receptor 1 in alcohol use disorder: Still a valid drug target? *Alcohol. Clin. Exp. Res.* **41**, 1986–1999 (2017).
74. C. A. Marcinkiewcz *et al*., Serotonin engages an anxiety and fear-promoting circuit in the extended amygdala. *Nature* **537**, 97–101 (2016).
75. J. J. Radley, P. E. Sawchenko, Evidence for involvement of a limbic paraventricular hypothalamic inhibitory network in hypothalamic-pituitary-adrenal axis adaptations to repeated stress. *J. Comp. Neurol.* **523**, 2769–2787 (2015).
76. W. E. Cullinan, D. R. Ziegler, J. P. Herman, Functional role of local GABAergic influences on the HPA axis. *Brain Struct. Funct.* **213**, 63–72 (2008).
77. B. S. McEwen, E. R. De Kloet, W. Rostene, Adrenal steroid receptors and actions in the nervous system. *Physiol. Rev.* **66**, 1121–1188 (1986).
78. M. Aronsson *et al*., Localization of glucocorticoid receptor mRNA in the male rat brain by in situ hybridization. *Proc. Natl. Acad. Sci. U.S.A.* **85**, 9331–9335 (1988).
79. R. S. Ahima, R. E. Harlan, Charting of type II glucocorticoid receptor-like immunoreactivity in the rat central nervous system. *Neuroscience* **39**, 579–604 (1990).
80. J. S. Kim, S. Y. Han, K. J. Iremonger, Stress experience and hormone feedback tune distinct components of hypothalamic CRH neuron activity. *Nat. Commun.* **10**, 5696 (2019).
81. G. P. McNally, J. P. Johansen, H. T. Blair, Placing prediction into the fear circuit. *Trends Neurosci.* **34**, 283–292 (2011).
82. J. E. LeDoux, J. Iwata, P. Cicchetti, D. J. Reis, Different projections of the central amygdaloid nucleus mediate autonomic and behavioral correlates of conditioned fear. *J. Neurosci.* **8**, 2517–2529 (1988).
83. P. Tovote *et al*., Midbrain circuits for defensive behaviour. *Nature* **534**, 206–212 (2016).
84. T. C. Watson, N. L. Cerminara, B. M. Lumb, R. Apps, Neural correlates of fear in the periaqueductal gray. *J. Neurosci.* **36**, 12707–12719 (2016).
85. National Research Council, *Guide for the Care and Use of Laboratory Animals* (National Academies Press, Washington, DC, ed. 8, 2011).
86. A. Ericsson, K. J. Kovács, P. E. Sawchenko, A functional anatomical analysis of central pathways subserving the effects of interleukin-1 on stress-related neuroendocrine neurons. *J. Neurosci.* **14**, 897–913 (1994).
87. J. J. Radley, C. M. Arias, P. E. Sawchenko, Regional differentiation of the medial prefrontal cortex in regulating adaptive responses to acute emotional stress. *J. Neurosci.* **26**, 12967–12976 (2006).
88. B. Roozendaal, B. Bohus, J. L. McGaugh, Dose-dependent suppression of adrenocortical activity with metyrapone: Effects on emotion and memory. *Psychoneuroendocrinology* **21**, 681–693 (1996).
89. R. T. LaLumiere, T. V. Buen, J. L. McGaugh, Post-training intra-basolateral amygdala infusions of norepinephrine enhance consolidation of memory for contextual fear conditioning. *J. Neurosci.* **23**, 6754–6758 (2003).
90. O. Yizhar, L. E. Fenno, T. J. Davidson, M. Mogri, K. Deisseroth, Optogenetics in neural systems. *Neuron* **71**, 9–34 (2011).
91. M. Mahn, M. Prigge, S. Ron, R. Levy, O. Yizhar, Biophysical constraints of optogenetic inhibition at presynaptic terminals. *Nat. Neurosci.* **19**, 554–556 (2016).
92. G. Paxinos, C. Watson, *The Rat Brain in Stereotaxic Coordinates* (Elsevier Academic, Amsterdam, 2007).
93. L. W. Swanson, *Brain Maps: Structure of the Rat Brain* (Elsevier, Amsterdam, 2004), p. 215.
94. F. Wang *et al*., RNAscope: A novel in situ RNA analysis platform for formalin-fixed, paraffin-embedded tissues. *J. Mol. Diagn.* **14**, 22–29 (2012).
95. M. J. Sharpe *et al*., Lateral hypothalamic GABAergic neurons encode reward predictions that are relayed to the ventral tegmental area to regulate learning. *Curr. Biol.* **27**, 2089–2100.e5 (2017).
96. X. Li *et al*., Incubation of methamphetamine craving is associated with selective increases in expression of Bdnf and trkb, glutamate receptors, and epigenetic enzymes in cue-activated fos-expressing dorsal striatal neurons. *J. Neurosci.* **35**, 8232–8244 (2015).